Journal of Alloys and Compounds 516 (2012) 49–52

Contents lists available at SciVerse ScienceDirect

Journal of Alloys and Compounds

journal homepage: www.elsevier.com/locate/jallcom

Upconversion photoluminescence properties of Er^{3+}-doped $Ba_xSr_{1-x}TiO_3$ powders with different phase structure

Lei Chen, Xiaolu Liang, Zhen Long, Xianhua Wei*

State Key Laboratory Cultivation Base for Nonmetal Composites and Functional Materials, Southwest University of Science and Technology, Mianyang 621010, PR China

ARTICLE INFO

Article history:
Received 19 October 2011
Received in revised form
22 November 2011
Accepted 24 November 2011
Available online 8 December 2011

Keywords:
Phase transition
Photoluminescence
Cross relaxation
Crystal field
Symmetry

ABSTRACT

The composition of Ba/Sr in $Ba_xSr_{1-x}TiO_3$ phosphors doped with Er^{3+} has been varied to investigate the effect of phase structure on the upconversion photoluminescence properties. XRD results suggest that phase transition from tetragonal to cubic phase occurs at room temperature near $x = 0.7$. Under the excitation of 980 nm laser, the quenching of green upconversion emission accompanied with enhancement of red relative emission intensity was observed with the decrease of x. It could be attributed to the decrease of the local symmetry around the Er^{3+} ion and the strengthening of the cross relaxation process, respectively. Additional, the smoother spectra shape in the cubic samples reveals the weaker influence of the more centrosymmetric crystal field. The upconversion mechanisms are also discussed in detail through laser power dependence.

1. Introduction

Upconversion (UC) luminescence of rare earth ions doped perovskite-structure materials has been investigated extensively in recent years due to their applications in UC phosphors, fluorescent labels for sensitive detection of biomolecules, flat panel displays and structure probe [1–8]. Among these rare earth ions, Er^{3+} ion as an active ion has drawn broad attention because it shows strong excited state absorption under the excitation of commercial low-cost 980 and 800 nm laser diodes [9,10]. It is well known that characteristic luminescence features of these materials are determined by the electronic structure of the doped rare earth, while the width and the relative intensity of the spectra frequently depend on the crystal symmetry of the host matrix. Ferroelectric and dielectric properties of perovskite oxides are sensitive to the crystal symmetry, which can be influenced by temperature change or controlled by ion solid solution. Obviously, the emission properties of Er^{3+} ion doped ferroelectrics should also be dependent on the two factors. For instance, temperature dependence of the luminescence properties has been reported in Er^{3+} doped $KNbO_3$ and $BaTiO_3$ systems [8,11]. However, it seems difficult to distinguish the contribution from phase transition and the intrinsic effect of temperature on PL properties [8]. Therefore, it is essential to correlate the phase transition and luminescence by changing the chemical composition of host at room temperature.

The luminescence properties of rare earths doped $Ba_xSr_{1-x}TiO_3$ (BST) materials have been widely studied in different forms including powders, ceramics and films [12–15]. In Pr^{3+} doped (Ba, Sr, Ca)TiO_3, the f–f transition probability was found to be enhanced due to lowering the point symmetry at the alkaline-earth site [15]. Unfortunately, the UC luminescence in relation to structure phase transitions of Er^{3+} doped BST has never been investigated yet. In this paper, different Ba/Sr ratios were designed to understand the UC mechanisms through laser power dependence and phase transition dependence of UC emissions.

2. Experimental

The composition of prepared samples was $Er_{0.01}(Ba_xSr_{1-x})_{0.985}TiO_3$ with $x = 0$, 0.5, 0.7, 0.9, 1. Here Er^{3+} was anticipated to occupy A-site by controlling (Ba + Sr)/Ti ratio, which had been proved to show a stronger UC photoluminescence [8]. Powders of high purity $BaCO_3$, $SrCO_3$, TiO_2 and Er_2O_3 were used as raw materials. Based on the above formulas, the starting powders with designed stoichiometric quantities were ball-milled in water for 24 h, then dried and calcined at 1100 °C for 8 h in air to produce the Er^{3+} doped $Ba_xSr_{1-x}O_3$ powders.

Phase purity and crystal structure of the obtained materials were analyzed by an X-ray diffractometer (XRD, Philips X'pert MPD Pro) utilizing copper K_α (wavelength: $\lambda = 1.5406$ Å) radiation. The surfaces morphologies of powders were characterized by a Hitachi S-4800 scanning electron microscope (SEM). The photoluminescence (PL) spectra were measured by the use of Hitachi F-4500 spectrofluorimeter. The excitation light for UC luminescence was a 980 nm laser diode with a maximum power output of 150 mw.

* Corresponding author. Tel.: +86 816 2419201.
E-mail address: weisansao@yahoo.com.cn (X. Wei).

0925-8388/$ – see front matter © 2011 Elsevier B.V. All rights reserved.
doi:10.1016/j.jallcom.2011.11.121

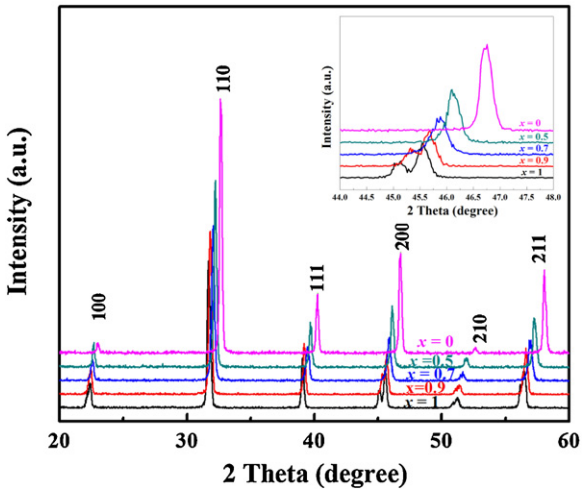

Fig. 1. XRD patterns of Er^{3+}:$Ba_xSr_{1-x}TiO_3$ powders synthesized at 1100 °C for 8 h.

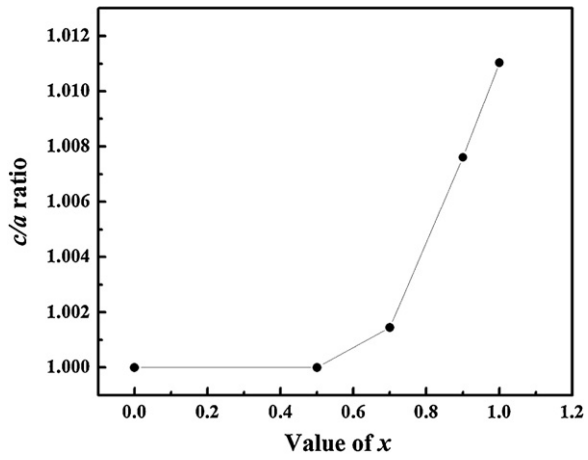

Fig. 2. c/a ratio as function of x values.

3. Results and discussion

Fig. 1 displays the XRD patterns of Er^{3+} doped $Ba_xSr_{1-x}TiO_3$ (x = 0, 0.5, 0.7, 0.9, 1.0) powders synthesized at 1100 °C for 8 h. Only the diffraction peaks from perovskite phase can be observed and Er_2O_3 was hardly examined from the XRD patterns, suggesting that Er was effectively doped into the host lattice. There are obvious shifts of the diffraction peak (2 0 0) between the Er^{3+} doped samples as shown in the inset of Fig. 1, meaning that $Ba_xSr_{1-x}TiO_3$ solid solutions are successfully synthesized. The strong peaks indicate the high crystalline of the as-prepared powders, which is very beneficial for obtaining bright luminescence. Additional, distinct splitting of cubic (2 0 0) into tetragonal (2 0 0) and (0 0 2) reflections at about 45° can be observed when the x value exceeds 0.7. To further investigate the variation of structures with the increase of x values, the tetragonality (c/a) of powders as a function of x is plotted as shown in Fig. 2. As x values varies from 0.5, 0.7, 0.9 to 1.0, the c/a ratio increases from 1.0, 1.001, 1.008 to 1.011, respectively. The result demonstrates that crystalline structure undergoes phase transition near x = 0.7, which is similar to the result reported by Kyômen et al. [15]. Thus, the rising c/a ratio as increasing x is expected to enhance the UC luminescence due to the decrease of the local symmetry around rare earth ions.

The SEM micrographs of Er^{3+} doped $Ba_xSr_{1-x}TO_3$ powders are shown in Fig. 3. All the samples have similar morphology. These images exhibit a narrow size distribution with a slight agglomerate phenomenon and their grain sizes show no distinct difference in the range of 0.3–0.5 μm. Therefore, the influence of grain size on the UC photoluminescence among these powder samples could be neglected.

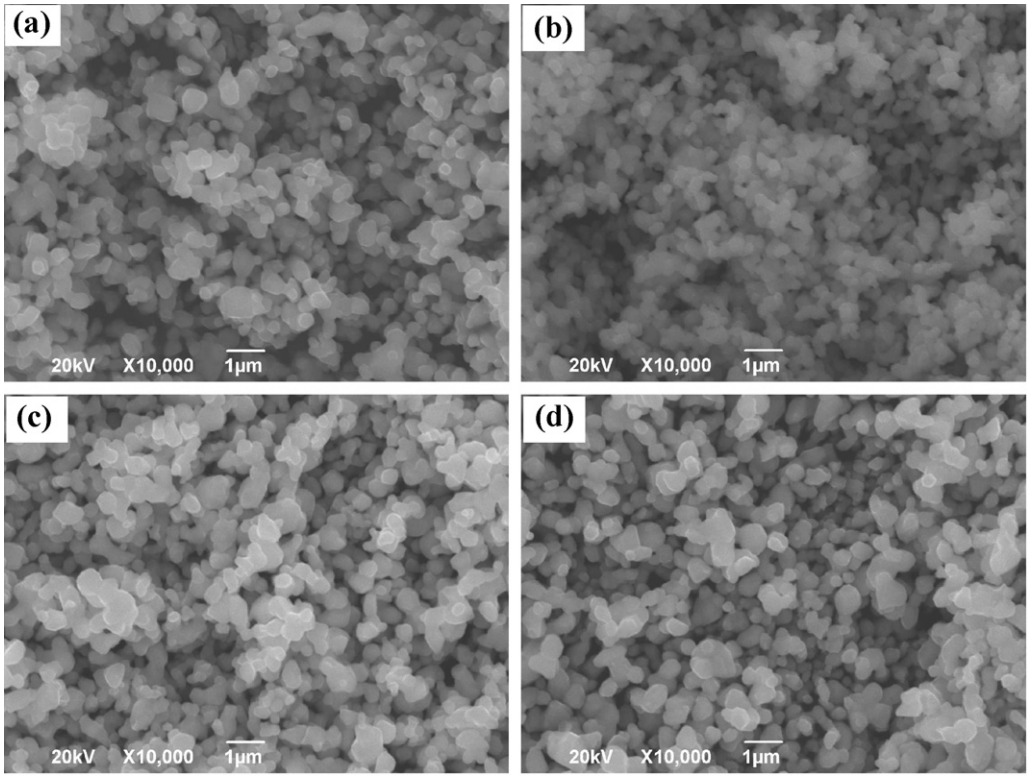

Fig. 3. Scanning electron micrographs of Er^{3+} doped $Ba_xSr_{1-x}TiO_3$ phosphors: (a) x = 1.0, (b) x = 0.9, (c) x = 0.7, (d) x = 0.5.

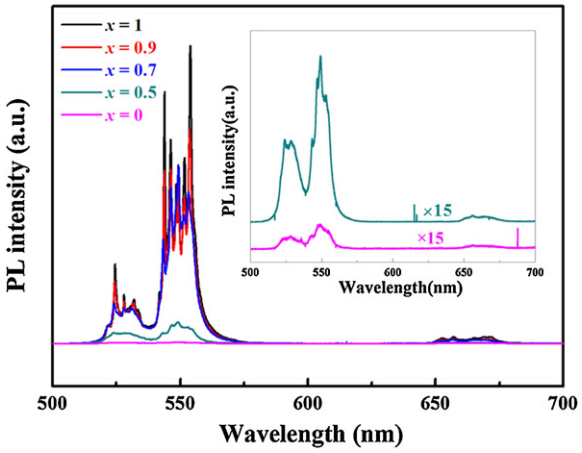

Fig. 4. Anti-Stokes emission spectra of Er^{3+}-doped $Ba_xSr_{1-x}TiO_3$ with different x values measured at room temperature.

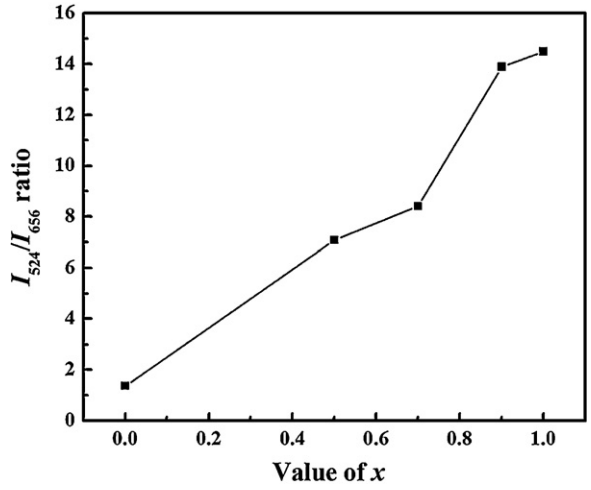

Fig. 5. The green-to-red intensity ratio as function of x values.

Fig. 4 shows the anti-stokes emission spectra of Er^{3+} doped $Ba_xSr_{1-x}TiO_3$ with different x values measured at room temperature. The typical UC emission consists of two strong green bands and a weak red band located at 528, 548 and 656 nm originating from the intra 4f–4f electronic transitions $^2H_{11/2}/^4S_{3/2} \rightarrow {}^4I_{15/2}$ and $^4F_{9/2} \rightarrow {}^4I_{15/2}$ of the Er^{3+} ions, respectively. Obvious level splits can be observed when the x value is more than 0.7, which can be attributed to the Stark splitting of the degenerate 4f levels under the strong crystal field [16]. The split is more remarkable with increasing x because of the larger asymmetric crystal field for the host material with larger tetragonality. The changes of spectral shapes also prove that phase transition occurs when x value is between 0.5 and 0.7. By contrast, there is no difference about the shapes in red UC emission, which reveals different underlying mechanism between the red emission and the green one. It is worth noting that the UC emission intensity at 528 nm of Er^{3+} doped $Ba_{0.7}Sr_{0.3}TiO_3$ is about 15 times higher than that of Er^{3+} doped $Ba_{0.5}Sr_{0.5}TiO_3$ under same excitation conditions. According to the quantum mechanical selection rules, the electric dipole transition between $4f^n$ levels is forbidden when a rare-earth ion is located at a centrosymmetric site. In the case of phase transition of Er:$Ba_xSr_{1-x}TiO_3$ with increasing x from cubic to tetragonal phase, it should be broken by the local crystal field of the rare earths [17]. Hence, the f–f transitions probability increases with the increase of x. Moreover, the green-to-red (I_{524}/I_{656}) ratio is also calculated for all the samples as shown in Fig. 5. It can be seen that the ratio is 1.370, 7.077, 8.402, 13.882 and 14.489 for $x = 0$, 0.5, 0.7, 0.9 and 1.0, respectively. The significant difference of green-to-red ratio could be understood by the extent of the local symmetry influence on the different emission bands [18]. According to the Judd–Ofelt theory, the green emission bands are mainly dominated by Ω_2 while the red are little affected by the parameter. Since the lower symmetry of the lanthanide ion sites usually contributes to the larger Ω_2, the enhancement of the ratio with the increase of x is attributed to the decrease of the symmetry surrounding Er^{3+} ions caused by the phase structure evolution of the BST host.

To better comprehend the mechanism which populate the ($^2H_{11/2}$, $^4S_{3/2}$) green- and ($^4F_{9/2}$) red-emitting levels, the relationships between the UC intensity and the pump power have been examined at 524 nm and 656 nm. According to the theoretical consideration of the mutiphoton absorption process, the relationship can be described as a power law:

$$I \propto P^n$$

where I is the intensity of UC photoluminescence, P is the pump laser power and n is the number of laser photons required. As shown in Fig. 6, the n values of 524 nm and 656 nm UC band are fitted to be 2.17 ± 0.02 and 1.60 ± 0.02 in Er^{3+} doped $Ba_{0.7}Sr_{0.3}TiO_3$ powders, respectively, while the n values of the two UC band are respectively 1.29 ± 0.02 and 1.08 ± 0.02 for Er^{3+} doped $Ba_{0.5}Sr_{0.5}TiO_3$ powders.

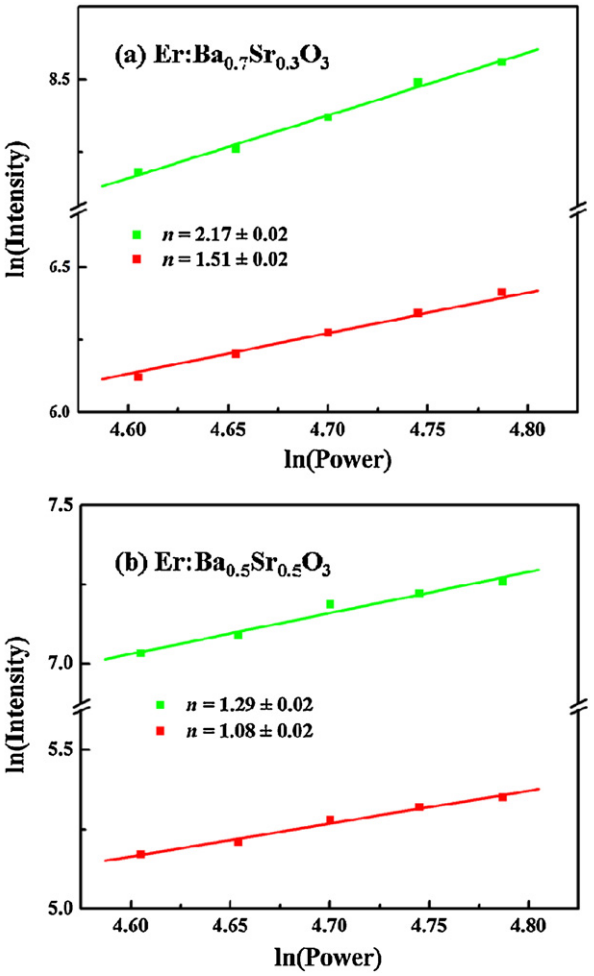

Fig. 6. Pump power dependence of the green and red emission of Er^{3+}-doped $Ba_{0.7}Sr_{0.3}TiO_3$ (a) and Er^{3+}-doped $Ba_{0.5}Sr_{0.5}TiO_3$ (b).

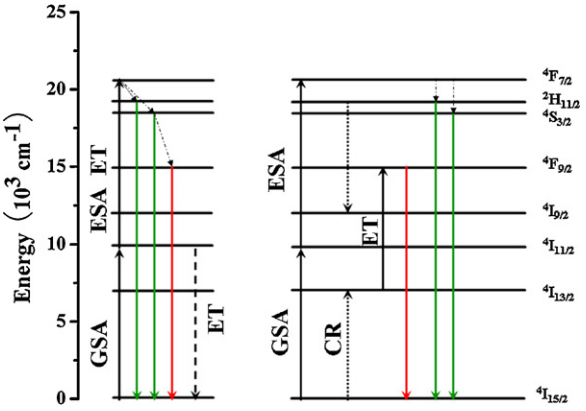

Fig. 7. Energy level diagrams of the Er^{3+} as well as the proposed UC mechanisms for the green and red emissions.

It is clear that the *n*-values are enhanced in tetragonal samples for both green and red emissions. Similar results have been reported by Huang and Hsieh [16] and Sun et al. [17], which could be ascribed to the change of local crystal field around Er^{3+} ions. Furthermore, the *n* values for green and red emissions are close to 2 in Er^{3+} doped $Ba_{0.7}Sr_{0.3}TiO_3$ powders, indicating two-photo processes contribute to the green and red UC emissions. On the other hand, the smaller slopes *n* of the red emission obtained for Er^{3+} doped $Ba_{0.5}Sr_{0.5}TiO_3$ samples suggest that it is a mixing process of one- and two-photon with one-photon process being dominant.

Fig. 7 sketches the energy level diagram of Er^{3+} and the probable UC mechanisms accounting for the green and red emissions under the 980 nm excitation. Er^{3+} ion is excited initially from the ground state $^4I_{15/2}$ to the $^4I_{11/2}$ state in the ground-state absorption (GSA) process. Through excited-state absorption (ESA) process, Er^{3+} ion is further excited to $^4F_{7/2}$ from the $^4I_{11/2}$ state. Subsequently, Er^{3+} ion then relaxes nonradiatively to the $^2H_{11/2}$ and $^4S_{3/2}$ levels by multi-phonon relaxation, from which the strong green $^2H_{11/2} \rightarrow {}^4I_{15/2}$ and $^4S_{3/2} \rightarrow {}^4I_{15/2}$ emissions occur. The above mechanism is a two-photo process, which is an agreement with the case of the green emissions in all samples. There could be another route which enhances the green emissions in Er^{3+} doped tetragonal samples. Through the process of ET accompanied with ESA, an excited ion relaxes from $^4I_{11/2}$ level to $^4I_{15/2}$ level nonradiatively and transfers the excitation energy to a neighboring ion in the same level, promoting the latter to $^4F_{7/2}$ level.

The red emission in tetragonal samples is mainly determined by a nonradiative relaxation from the $^4S_{3/2}$ excited state to $^4F_{9/2}$ level. Due to the large energy gap between $^4S_{3/2}$ and $^4F_{9/2}$ levels, the nonradiative relaxation probability is quite low [19]. As a result, the intensity of the red emission is weaker than that of green emission. However, from the enhanced population of the $^4F_{9/2}$ state and the smaller slopes *n* of the red emission in cubic samples, it could be inferred that the red emission is mainly dominated by the cross relaxation, i.e. $^2H_{11/2} + {}^4I_{15/2} \rightarrow {}^4I_{9/2} + {}^4I_{13/2}$. Hence, the Er^{3+} ions at $^4I_{13/2}$ state through ET process populate the $^4F_{9/2}$ state, primarily enhancing the red intensity [8]. In other words, it is a one-photo process dominating the red emission in Er:$Ba_{0.5}Sr_{0.5}TiO_3$ samples.

4. Conclusions

In conclusion, effects of phase transition designed by different Ba/Sr ratio on the photoluminescence properties of Er^{3+} doped $Ba_xSr_{1-x}TiO_3$ powders are reported in this paper. The results demonstrate that phase structure plays an important role in both the shape of PL spectra and the intensity of PL. As increasing *x* values, the samples tend to become tetragonal phase with great enhancement of green emission and obvious level splits due to the low local symmetry of crystal field. Different green-to-red ratio should be attributed to the local symmetry influence on the emission bands. The detailed upconversion mechanisms accounting for green and red emissions are discussed. The results indicate that it could be useful in the structure probe to detect the phase transition.

Acknowledgment

This work was supported by National Natural Science Foundation of China (No. 50802078).

References

[1] Y.X. Liu, W.A. Pisarski, S.J. Zeng, C.F. Xu, Q.B. Yang, Opt. Express 17 (2009) 9089.
[2] H.X. Zhang, C.H. Kam, Y. Zhou, X.Q. Han, S. Buddhudu, Q. Xiang, Y.L. Lam, Appl. Phys. Lett. 77 (2000) 609.
[3] J.H. Zeng, J. Su, Z.H. Li, R.X. Yan, Y.D. Li, Adv. Mater. 17 (2005) 2119.
[4] Y. Pan, Q. Su, H. Xu, T. Chen, W. Ge, C. Yang, M. Wu, J. Solid State Chem. 174 (2003) 69.
[5] Z.L. Fu, B.K. Moon, H.K. Yang, J.H. Jeong, J. Phys. Chem. C 112 (2008) 5724.
[6] A. Polman, Physica B 300 (2001) 78.
[7] N.M. Samsuri, A.K. Zamzuri, M.H. Al-Mansoori, A. Ahmad, M.A. Mahdi, Opt. Express 16 (2008) 16475.
[8] Y. Zhang, J.H. Hao, C.L. Mak, X.H. Wei, Opt. Express 19 (2011) 1824.
[9] H. Lin, G. Meredith, S. Jiang, X. Peng, T. Luo, N. Peyghambarian, E. Yue-Bun Pun, J. Appl. Phys. 93 (2003) 186.
[10] H. Guo, N. Dong, M. Yin, W.P. Zhang, L.R. Lou, S.D. Xia, J. Alloys Compd. 415 (2006) 280.
[11] X.Q. Chen, Z.K. Liu, Q. Sun, M. Ye, F.P. Wang, Opt. Commun. 284 (2011) 2046.
[12] C. Shen, Q. Liu, Q.F. Liu, Mater. Sci. Eng. B 111 (2004) 31.
[13] C.B. Samantaray, M.L. Nanda Goswami, D. Bhattacharya, S.K. Ray, H.N. Acharya, Mater. Lett. 58 (2004) 2299.
[14] S.Y. Kuo, W.F. Hsieh, J. Vac. Sci. Technol. A 23 (2005) 768.
[15] T. Kyômen, R. Sakamoto, N. Sakamoto, S. Kunugi, M. Itoh, Chem. Mater. 17 (2005) 3200.
[16] T.C. Huang, W.F. Hsieh, J. Fluoresc. 19 (2009) 511.
[17] Q. Sun, X.Q. Chen, Z.K. Liu, F.P. Wang, Z.H. Jiang, C. Wang, J. Alloys Compd. 509 (2011) 5336.
[18] J.H. Hao, Y. Zhang, X.H. Wei, Angew. Chem. Int. Ed. 50 (2011) 6876.
[19] F. Gao, G.H. Wu, H. Zhou, D.H. Bao, J. Appl. Phys. 106 (2009) 126104.